Frequency Response Data-Driven LPV Controller Synthesis for MIMO Systems

Tom Bloemers, Tom Oomen, *Senior Member, IEEE*, and Roland Tóth, *Senior Member, IEEE*

***Abstract*—The linear parameter-varying framework enables systematic control design approaches to meet increasing performance requirements and complexity of systems. The aim of this letter is to develop local frequency response data-based analysis and synthesis conditions for multiple-input multiple-output linear parameter-varying systems to facilitate fast tuning. Key advantages are local stability and performance guarantees and a global controller parameterization. The effectiveness of the proposed methods are evaluated based on a simulation example.**

***Index Terms*—Identification for control, linear parameter-varying systems.**

I. Introduction

USING frequency response functions (FRFs) to manually design controllers directly from measurement data is often used in the industry [1]. FRF estimates provide accurate nonparametric system descriptions, which are relatively fast and inexpensive to obtain [2]. This has motivated the development of classical frequency-domain control design techniques, based on graphical tools including Bode plots and Nyquist diagrams with efficient guiding rules and insight.

Data-driven control design techniques based on FRF estimates provide systematic tools to synthesize linear time-invariant (LTI) controllers. Beyond classical techniques, [3], extensions include more general control structures with a focus on $\mathcal{H}_\infty$-performance [4]. The $\mathcal{H}_\infty$ framework enables the incorporation of model uncertainties in the control design, which has led to the synthesis of stabilizing controllers that achieve robust stability and performance with respect to plant variations [5], [6]. However, this comes at the cost of performance. While these results are confined to the LTI case, the recent push for performance necessitates the direct addressing of nonlinearities, e.g., position dependency.

The concept of linear parameter-varying (LPV) systems provides a systematic framework for synthesis and analysis of gain-scheduled controllers for nonlinear systems [7], overcoming limitations of robust LTI controllers. LPV systems are characterized by a linear relation between the input-output (IO) signals. Unlike LTI systems, this map can change over time based on a measurable time-varying signal. This so-called scheduling signal can be used to describe operating condition-dependent dynamics or effectively embedding nonlinear dynamics in the solution set of an LPV system [8]. The LPV framework is supported with well-developed model-based control and identification approaches [8], [9].

Designing LPV controllers directly from measurement data is receiving increased interest. While time-domain approaches have been developed, e.g., [10], frequency domain methods [11], [12] mainly focus on single-input single-output (SISO) LPV systems. Common drawbacks of these methods include conservative stability and performance constraints, and limited freedom in the controller parameterization. A practically well-applicable method has been developed in [13], [14] overcoming these limitations. However, the extension to multiple-input multiple-output (MIMO) systems remains difficult because of the non-commutative nature of multivariable systems [15].

Based on recent integral quadratic constraint (IQC) results [16], [17], in this letter we present a novel method to design MIMO LPV controllers directly from frequency-domain measurement data. Key advantages are the local stability and performance guarantees and a global LPV controller parameterization that allows shaping of the poles and zeros based on local frequency-domain information.

The main contribution of this letter is

- C1 LPV controller synthesis method for unstable MIMO plants, using only frequency-domain measurement data, with local stability and performance guarantees.

This is achieved by the following sub-contributions.

- C2 Development of local LPV frequency-domain IQC stability and performance analysis conditions.

Manuscript received September 14, 2021; revised November 27, 2021; accepted December 16, 2021. Date of publication December 31, 2021; date of current version January 25, 2022. This work was supported in part by the European Research Council (ERC) through the European Union's Horizon 2020 Research and Innovation Programme under Grant 714663, and in part by the Ministry of Innovation and Technology NRDI Office within the framework of the Autonomous Systems National Laboratory Program. Recommended by Senior Editor V. Ugrinovskii. *(Corresponding author: Tom Bloemers.)*

Tom Bloemers is with the Control Systems Group, Department of Electrical Engineering, Eindhoven University of Technology, 5612 AZ Eindhoven, The Netherlands (e-mail: t.a.h.bloemers@tue.nl).

Tom Oomen is with the Control Systems Technology, Department of Mechanical Engineering, Eindhoven University of Technology, 5612 AZ Eindhoven, The Netherlands, and also with the Delft Center for Systems and Control, Department of faculty 3mE, Delft University of Technology, 2628 CD Delft, The Netherlands (e-mail: t.a.e.oomen@tue.nl).

Roland Tóth is with the Control Systems Group, Department of Electrical Engineering, Eindhoven University of Technology, 5612 AZ Eindhoven, The Netherlands, and also with the Systems and Control Laboratory, Institute for Computer Science and Control, 1111 Budapest, Hungary (e-mail: r.toth@tue.nl).

Digital Object Identifier 10.1109/LCSYS.2021.3139734

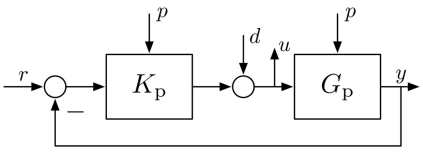

Fig. 1. Feedback interconnection of the plant G_p and controller K_p, dependent on the scheduling signal.

C3 Development of a locally stable LPV frequency-domain controller initialization algorithm.

Additional to the preliminary results in [14], a connection to dissipativity theory is established through the IQC theory presented in [17]. This allows for the more general notion of quadratic performance such as passivity, $\mathcal{H}_2$, $\mathcal{H}_\infty$, etc. The results are evaluated based on a simulation example. Although the theory presented in this letter is in continuous-time, discrete-time results follow analogously, see [18].

Notation: $\mathbb{C}^+$ denotes the open right-half complex plane and $\mathbb{C}^0 := i\mathbb{R} \cup \{\infty\}$ denotes the extended imaginary axis. $\mathcal{L}_2$ denotes the space of square integrable functions. $\mathcal{RL}_\infty$ and $\mathcal{RH}_\infty \subset \mathcal{RL}_\infty$ are sets of real-rational and proper transfer functions analytic on $\mathbb{C}^0$ and $\mathbb{C}^0 \cup \mathbb{C}^+$, respectively. The pair $\{N, D\}$ is a Right Coprime Factorization (RCF) of P if D is invertible, $N, D \in \mathcal{RH}_\infty^{\cdot\times\cdot}$, $P = ND^{-1}$ and $\exists X_r, Y_r \in \mathcal{RH}_\infty^{\cdot\times\cdot}$ such that the Bézout identity $X_rD + Y_rN = I$ holds. Similiarly, $\{\tilde{N}, \tilde{D}\}$ is a Left Coprime Factorization (LCF) $P = \tilde{D}^{-1}\tilde{N}$ if $\tilde{D}$ is invertible, $\tilde{N}, \tilde{D} \in \mathcal{RH}_\infty^{\cdot\times\cdot}$ and $\exists X_l, Y_l \in \mathcal{RH}_\infty^{\cdot\times\cdot}$ such that $\tilde{D}X_l + \tilde{Y}N_l = I$. If $G = G^* \in \mathcal{RL}_\infty^{\cdot\times\cdot}$, then $G \succ 0$ on $\mathbb{C}^0$ implies that G satisfies the frequency domain inequality (FDI) $G(i\omega) \succ 0$ for all $\omega \in \mathbb{R} \cup \{\infty\}$.

II. Problem Formulation

A. Linear Parameter-Varying Systems

Consider the MIMO continuous-time (CT) LPV system

$$\mathcal{G} : \begin{cases} \dot{x}(t) = A(p(t))x(t) + B(p(t))u(t), \\ y(t) = C(p(t))x(t) + D(p(t))u(t). \end{cases} \tag{1}$$

Here, $x : \mathbb{R} \to \mathbb{R}^{n_x}$ is the state variable, $u : \mathbb{R} \to \mathbb{R}^{n_u}$ is the input signal, $y : \mathbb{R} \to \mathbb{R}^{n_y}$ is the output signal and $p : \mathbb{R} \to \mathbb{P} \subseteq \mathbb{R}^{n_p}$ the scheduling variable. If the scheduling signal $p(t) \equiv \mathrm{p}$ is constant (1) becomes LTI, i.e.,

$$G_\mathrm{p} : \begin{cases} \dot{x}(t) = A(\mathrm{p})x(t) + B(\mathrm{p})u(t), \\ y(t) = C(\mathrm{p})x(t) + D(\mathrm{p})u(t). \end{cases} \tag{2}$$

For a given $\mathrm{p} \in \mathbb{P}$, (2) describes the local behavior of (1). We define the Fourier transform of (2) by

$$Y(i\omega) = G_\mathrm{p}(i\omega)U(i\omega), \tag{3}$$

where $G_\mathrm{p}(i\omega)$ represents the frozen frequency response function (fFRF) of (1) for constant $p(t) \equiv \mathrm{p} \in \mathbb{P}$. Similarly, $\mathcal{K}$ denotes an LPV controller with local behavior K_p.

B. Problem Formulation

Consider the four-block closed-loop map $T(G_\mathrm{p}, K_\mathrm{p}) : \mathrm{col}(r, d) \mapsto \mathrm{col}(y, u)$ defined by

$$T(G_\mathrm{p}, K_\mathrm{p}) = \begin{pmatrix} K_\mathrm{p} \\ I \end{pmatrix} (I + G_\mathrm{p}K_\mathrm{p})^{-1} \begin{pmatrix} G_\mathrm{p} & I \end{pmatrix} \tag{4}$$

corresponding to the feedback interconnection in Figure Fig. 1, where $G_\mathrm{p} \in \mathcal{RL}_\infty^{n_y \times n_u}$ denotes the local plant for $p(t) \equiv \mathrm{p}$ and $K_\mathrm{p} \in \mathcal{RL}_\infty^{n_u \times n_y}$ the controller. The interconnection in Figure Fig. 1 is internally stable if and only if (4) is stable.

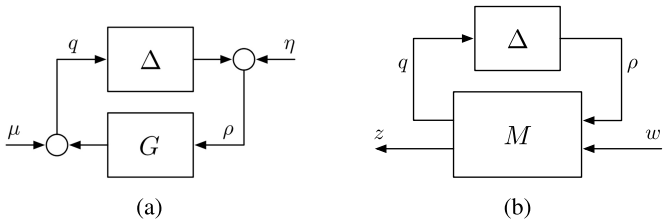

Fig. 2. Feedback interconnection for robust stability (a) and Performance (b) analysis.

The problem addressed in this letter is to synthesize an LPV controller $\mathcal{K}$ directly from fFRF data such that for any $\mathrm{p} \in \mathbb{P}$, the local aspect of the plant G_p and of the controller K_p satisfy the following requirements:

R1 The map $T(G_\mathrm{p}, K_\mathrm{p})$ is internally stable.

R2 The map $T(G_\mathrm{p}, K_\mathrm{p})$ achieves quadratic performance.

Here, quadratic performance refers to performance with respect to a pre-defined quadratic measure, for example a bound on the $\mathcal{L}_2$-gain. This is clarified further in Section III-A. Consider the fFRF data $\mathcal{D}_{N,\mathrm{p}_\ell} = \{G_\mathrm{p}(i\omega_k), p_\ell\}_{k=1}^{N}$, obtained at the constant scheduling points $\mathcal{P} = \{\mathrm{p}_\ell\}_{\ell=1}^{N_\mathrm{loc}} \subset \mathbb{P}$. The frequencies are assumed to be sufficiently dense such that is suffices to check a finite number of discrete points only to draw conclusions on the underlying continuous curve. As IQCs form the basis of our results, we give a short introduction to them based on [18] in the next section.

III. Integral Quadratic Constraints

A. Considered Problem Setting

Consider an uncertain dynamic system corresponding to the interconnection in Figure Fig. 2(a), where

$$q = G\rho + \mu, \tag{5a}$$

$$\rho = \Delta(q) + \eta. \tag{5b}$$

Here, $G \in \mathcal{RH}_\infty^{n_q \times n_\rho}$ is the nominal LTI plant, $\Delta : \mathcal{L}_2^{n_q} \to \mathcal{L}_2^{n_\rho}$ is a causal and bounded operator, and $\mu \in \mathcal{L}_2^{n_q}$ and $\eta \in \mathcal{L}_2^{n_\rho}$ are exogenous input disturbances. Typically, Δ describes the trouble-making component, e.g., uncertain, time-varying, or nonlinear dynamics, which takes values in a pre-defined class $\mathbf{\Delta}$. The interconnection in Figure Fig. 2(a) separates the uncertain component from a nominal LTI system. Analysis of (5) follows a similar separation by considering G and $\mathbf{\Delta}$ separately through an IQC and an FDI, respectively. We introduce the following definitions [17].

Definition 1 (Well-Posedness): The feedback interconnection (5) is well-posed if for each $\mathrm{col}(\mu, \eta) \in \mathcal{L}_2^{n_q+n_\rho}$ there exists a unique response $\mathrm{col}(q, \rho) \in \mathcal{L}_2^{n_q+n_\rho}$ such that $\mathrm{col}(q, \rho)$ depends causally on $\mathrm{col}(\mu, \eta)$.

Definition 2 (Stability): The feedback interconnection (5) is stable if it is well-posed and the $\mathcal{L}_2$-gain of the map $\mathrm{col}(\mu, \eta) \mapsto \mathrm{col}(q, \rho)$ is bounded.

Definition 3: (Robust Stability): The feedback interconnection (5) is robustly stable if it is stable for all $\Delta \in \mathbf{\Delta}$.

B. Integral Quadratic Constraints

Two signals $\rho \in \mathcal{L}_2^{n_\rho}$ and $q \in \mathcal{L}_2^{n_q}$ are said to satisfy the IQC defined by the multiplier $\Pi : i\mathbb{R} \to \mathbb{C}^{(n_q+n_\rho)\times(n_q+n_\rho)}$ if

$$\int_{-\infty}^{\infty} \begin{pmatrix} \hat{q}(i\omega) \\ \hat{\rho}(i\omega) \end{pmatrix}^* \Pi(i\omega) \begin{pmatrix} \hat{q}(i\omega) \\ \hat{\rho}(i\omega) \end{pmatrix} d\omega \geq 0. \tag{6}$$

Here (6) describes the energy distribution along the spectrums of (q, ρ). In general, Π can be any measurable bounded Hermitian-valued function. By Parseval's theorem, the frequency-domain IQC is equivalent to the time-domain

$$\mathcal{I}(\Pi, q, \rho) := \left\langle \begin{pmatrix} q \\ \rho \end{pmatrix}, \Pi \begin{pmatrix} q \\ \rho \end{pmatrix} \right\rangle \geq 0, \tag{7}$$

where Π is also used to denote the time-domain operator equivalent to multiplication with Π in the frequency domain. When $\rho = \Delta(q)$ and there is a Π such that $\mathcal{I}(\Pi, q, \Delta(q)) \geq 0$, $\forall q \in \mathcal{L}_2^{n_q}$, it is possible to describe energy relations between the inputs and outputs of Δ. For stability, consider the IQC theorem of [16]:

Theorem 1: Let $G \in \mathcal{RH}_\infty^{n_q \times n_\rho}$ and $\Delta \in \mathbf{\Delta}$. Assume that

1) for all $\tau \in [0, 1]$ the feedback interconnection (5) is well-posed for Δ replaced by $\tau\Delta$; and
2) for all $\tau \in [0, 1]$ and some $\Pi \in \mathcal{RL}_\infty^{(n_q+n_\rho)\times(n_q+n_\rho)}$ the IQC (6) is satisfied for Δ replaced by $\tau\Delta$.

Then, the feedback interconnection (5) is robustly stable if there exists some $\Pi \in \mathcal{RL}_\infty^{(n_q+n_\rho)\times(n_q+n_\rho)}$ for which the following FDI is satisfied:

$$\begin{pmatrix} G(i\omega) \\ I \end{pmatrix}^* \Pi(i\omega) \begin{pmatrix} G(i\omega) \\ I \end{pmatrix} \prec 0, \ \forall \omega \in \mathbb{R} \cup \{\infty\}. \tag{8}$$

In the sequel, we will express the FDI $X(i\omega) \prec 0$, $\forall \omega \in \mathbb{R} \cup \{\infty\}$ as $X \prec 0$ on $\mathbb{C}^0$.

C. Robust Stability Analysis

To handle large uncertainty classes, we construct the family of IQC-multipliers $\mathbf{\Pi} \subset \mathcal{RL}_\infty^{(n_q+n_\rho)\times(n_q+n_\rho)}$ such that the IQC (6) holds for all $\Pi \in \mathbf{\Pi}$ and for all $\Delta \in \mathbf{\Delta}$. For technical reasons, $\mathbf{\Delta}$ is assumed to be star-shaped, i.e.,

Assumption 1: $\Delta \in \mathbf{\Delta}$ implies that $\tau\Delta \in \mathbf{\Delta}$ for all $\tau \in [0, 1]$.

Later, we will drop this assumption. As stated in [17], Theorem 1 can be used for robust stability analysis:

Corollary 1: Assume that, for all $\Delta \in \mathbf{\Delta}$,

1) the feedback interconnection (5) is well-posed; and
2) for all $\Pi \in \mathbf{\Pi}$, the IQC (6) is satisfied.

Then, the interconnection (5) is robustly stable if there exists a $\Pi \in \mathbf{\Pi}$ for which the following FDI is satisfied on $\mathbb{C}^0$:

$$\begin{pmatrix} G \\ I \end{pmatrix}^* \Pi \begin{pmatrix} G \\ I \end{pmatrix} \prec 0. \tag{9}$$

D. Robust Performance Analysis

For the analysis of robust performance, we augment the feedback interconnection in Figure Fig. 2(a) with a performance channel as depicted in Figure Fig. 2(b). The feedback interconnection is is now defined through the linear fractional representation (LFR) such that $w \mapsto z : \mathcal{F}_u(\Delta(q), M)$.

$$\begin{pmatrix} q \\ z \end{pmatrix} = \begin{pmatrix} M_{q\rho} & M_{qw} \\ M_{z\rho} & M_{zw} \end{pmatrix} \begin{pmatrix} \rho \\ w \end{pmatrix}, \qquad \rho = \Delta(q). \tag{10}$$

where $M \in \mathcal{RH}_\infty^{(n_q+n_z)\times(n_\rho+n_w)}$ is the nominal plant. We assume that (10) is well-posed for all $\Delta \in \mathbf{\Delta}$. We intend to impose performance criteria on $w \mapsto z$ through the IQC

$$\mathcal{I}_d(\Pi_d, z, w) := \left\langle \begin{pmatrix} z \\ w \end{pmatrix}, \Pi_d \begin{pmatrix} z \\ w \end{pmatrix} \right\rangle \leq \epsilon \|w\|^2, \tag{11}$$

where $\epsilon > 0$ and Π_d is a frequency dependent performance index confined to the set

$$\mathbf{\Pi}_d \subset \left\{ \Pi_d \in \mathcal{RL}_\infty^{(n_z+n_w)\times(n_z+n_w)} \;\middle|\; \Pi_{d11} \succcurlyeq 0 \text{ on } \mathbb{C}^0 \right\}. \tag{12}$$

The family $\mathbf{\Pi}_d$ represents a measure of quadratic performance such as passivity, $\mathcal{L}_2$ or $\mathcal{H}_2$ performance. Next, we extend Corollary 1 for robust performance [18].

Definition 4 (Robust Performance): The feedback interconnection (10) achieves robust performance w.r.t. (12) if it is robustly stable and if there exists some $\Pi_d \in \mathbf{\Pi}_d$ such that (11) holds for all trajectories of (10) generated by $w \in \mathcal{L}_2^{n_w}$.

Corollary 2: Assume that, for all $\Delta \in \mathbf{\Delta}$,

1) the LFR (10) is well-posed; and
2) for all $\Pi \in \mathbf{\Pi}$ the IQC (6) is satisfied.

Then, the interconnection (10) is robustly stable and achieves robust performance if there exist $\Pi \in \mathbf{\Pi}$ and $\Pi_d \in \Pi_d$ which satisfy the following FDI on $\mathbb{C}^0$:

$$\left(\begin{array}{cc|c} M_{q\rho} & M_{qw} & \\ I & 0 & \\ \hline M_{z\rho} & M_{zw} & \\ 0 & I & \end{array}\right)^* \left(\begin{array}{c|c} \Pi & 0 \\ \hline 0 & \Pi_d \end{array}\right) \left(\begin{array}{cc|c} M_{q\rho} & M_{qw} & \\ I & 0 & \\ \hline M_{z\rho} & M_{zw} & \\ 0 & I & \end{array}\right) \prec 0. \tag{13}$$

If $\rho = \Delta(q) = \Delta q$, then the IQC (6) reads as

$$\int_{-\infty}^{\infty} \hat{q}^*(i\omega) \begin{pmatrix} I \\ \hat{\Delta}(i\omega) \end{pmatrix}^* \Pi(i\omega) \begin{pmatrix} I \\ \hat{\Delta}(i\omega) \end{pmatrix} \hat{q}(i\omega) d\omega \geq 0,$$

which in turn is satisfied if the following FDI holds:

$$\begin{pmatrix} I \\ \hat{\Delta}(i\omega) \end{pmatrix}^* \Pi(i\omega) \begin{pmatrix} I \\ \hat{\Delta}(i\omega) \end{pmatrix} \succcurlyeq 0 \text{ on } \mathbb{C}^0. \tag{14}$$

Remark 1: Since $\Pi_{d11} \succcurlyeq 0$, (13) implies (9) for G replaced by $M_{q\rho}$. Hence, by Corollary 1, (10) is robustly stable.

IV. Four-Block IQC Analysis

In this section, stability and performance conditions are presented for the considered four-block problem, satisfying Requirements II-B and II-B. This forms Contribution I.

Assume that for all frozen $p \in \mathbb{P}$, the plant admits the LCF $G_p = D_{G_p}^{-1} N_{G_p}$ and the controller admits the RCF $K_p = N_{K_p} D_{K_p}^{-1}$. Then for all $p \in \mathbb{P}$, the map $w \mapsto z : T(G_p, K_p)$ in Figure Fig. 1 can be equivalently expressed by

$$T(G_p, K_p) = N_z D^{-1} N_w, \tag{15}$$

with

$$N_z = \begin{pmatrix} N_{K_p} \\ D_{K_p} \end{pmatrix}, \ N_w = \begin{pmatrix} N_{G_p} & D_{G_p} \end{pmatrix}, \ D = N_w N_z. \tag{16}$$

Note that in (16) the dependency on p is dropped for brevity. This parameterization allows for unstable subsystems within the IQC framework as is further exploited in the next section.

A. Reformulated Representation

With controller synthesis in mind, the main difficulty in (15) is the nonlinear appearance of the controller factors N_{K_p} and D_{K_p}. For that reason, we represent (15) by the following LFR such that $w \mapsto z : T(G_\mathrm{p}, K_\mathrm{p}) = \mathcal{F}_u(\Delta, M)$, with

$$M = \begin{pmatrix} (I_{n_y} - D) & (I_{n_y} - D)N_\mathrm{w} \\ N_\mathrm{z} & N_\mathrm{z}N_\mathrm{w} \end{pmatrix}, \quad \Delta = I_{n_y}. \tag{17}$$

Here, Δ does not represent a usual uncertainty, but a known quantity that results in an LFR of (15). Next, we exploit this specific LFR to obtain IQC analysis and synthesis conditions.

Remark 2: Even though the uncertainty singleton (17) violates Assumption 1, the IQC theory presented can be applied without modifications as mentioned in [17, Chapter 2.10.1].

B. Four-Block IQC Multipliers

Consider the set of all LTI real full-block operators $p = \Delta q$ defined by $p(t) = \tilde{\Delta}(\delta)q(t)$. Here, δ takes values in the polytope consisting of the single generator $\Lambda := \mathrm{co}\{\delta^1\} = \mathrm{co}\{1\}$. This corresponds to (17) and confines Δ to the singleton

$$\mathbf{\Delta}_{\mathrm{lti,re,fb}} := \left\{ \tilde{\Delta}(\delta) \;\middle|\; \delta \in \Lambda \right\}. \tag{18}$$

We can now state that the IQC (6) is satisfied for all $\Delta \in \mathbf{\Delta}_{\mathrm{lti,re,fb}}$ with $\Pi = \Pi^* \in \mathcal{RL}_\infty^{(n_q+n_\rho)\times(n_q+n_\rho)}$, if

$$\begin{pmatrix} I_{n_q} \\ \tilde{\Delta}(\delta^1) \end{pmatrix}^\top \Pi(i\omega) \begin{pmatrix} I_{n_q} \\ \tilde{\Delta}(\delta^1) \end{pmatrix} \succcurlyeq 0 \text{ on } \mathbb{C}^0, \tag{19a}$$

$$\begin{pmatrix} 0_{n_q} \\ I_{n_\rho} \end{pmatrix}^\top \Pi(i\omega) \begin{pmatrix} 0_{n_q} \\ I_{n_\rho} \end{pmatrix} \preccurlyeq 0 \text{ on } \mathbb{C}^0, \tag{19b}$$

and hence, the family of IQC multipliers reads as

$$\mathbf{\Pi}_{\mathrm{lti,re,fb}} := \left\{ \Pi \in \mathcal{RL}_\infty^{(n_q+n_\rho)\times(n_q+n_\rho)} \;\middle|\; (19) \right\}. \tag{20}$$

A proof follows by combining (6) with (19).

C. Four-Block Analysis Problem

In this subsection, we present analysis conditions to assess locally the quadratic performance of $T(G_\mathrm{p}, K_\mathrm{p})$ w.r.t. $\mathbf{\Pi}_\mathrm{d}$, constituting to Contribution I. Applying Corollary 2 to the LFR (17) results in the performance analysis conditions

$$\left(\begin{array}{cc} M_{\mathrm{q}\rho} & M_{\mathrm{qw}} \\ I & 0 \\ \hline M_{\mathrm{z}\rho} & M_{\mathrm{zw}} \\ 0 & I \end{array}\right)^* \left(\begin{array}{cc|c} \Pi & & 0 \\ & & \\ \hline 0 & & \Pi_\mathrm{d} \end{array}\right) \left(\begin{array}{cc} M_{\mathrm{q}\rho} & M_{\mathrm{qw}} \\ I & 0 \\ \hline M_{\mathrm{z}\rho} & M_{\mathrm{zw}} \\ 0 & I \end{array}\right) \prec 0,$$

$$\Pi \in \mathbf{\Pi}_{\mathrm{lti,re,fb}}, \quad \Pi_\mathrm{d} \in \mathbf{\Pi}_\mathrm{d}, \quad \forall \mathrm{p} \in \mathbb{P}, \quad \text{on } \mathbb{C}^0. \tag{21}$$

When considering the data $\mathcal{D}_{N,\mathrm{p}_\ell}$, with LCF $G_\mathrm{p} = D_{G_\mathrm{p}}^{-1} N_{G_\mathrm{p}}$ and RCF $K_\mathrm{p} = N_{K_\mathrm{p}} D_{K_\mathrm{p}}^{-1}$, the FDIs (21) result in a convex optimization problem in the variables Π and Π_d.

Taking for example the performance index

$$\mathbf{\Pi}_\mathrm{d} := \left\{ \mathrm{diag}(\gamma^{-1} I, -\gamma I) \in \mathbb{S}^{n_z+n_w} \;\middle|\; 0 < \gamma \leq \gamma_b \right\}, \tag{22}$$

with $\gamma_b > 0$ implies a bound on the induced $\mathcal{L}_2$-gain, i.e., $\|\mathcal{F}_u(\Delta, M)\|_\infty < \gamma_b$. The choice of (22) allows to minimize over γ subject to (21) to obtain an upper bound on the worst-case $\mathcal{L}_2$-gain from w to z. Although (21) is convex for analysis, it is non-convex for synthesis due to the nonlinear relation between the IQC multiplier and the controller.

Algorithm 1: IQC Synthesis Iterations

1. Set $\kappa = 0$. Initialize the controller $\{N_{K_\mathrm{p}}^{(\kappa)}, D_{K_\mathrm{p}}^{(\kappa)}\}$.
2. **while** Π_d *converges and* $\kappa \leq \kappa_{\max}$ **do**
3. Set $\kappa = \kappa + 1$.
4. Multiplier optimization: Given $\{N_{K_\mathrm{p}}^{(\kappa)}, D_{K_\mathrm{p}}^{(\kappa)}\}$, solve (21) and obtain $\{\Pi^{(\kappa)}, \Pi_\mathrm{d}^{(\kappa)}\}$.
5. Controller synthesis: Given $\{\Pi^{(\kappa)}\}$, solve (24) and obtain $\{N_{K_\mathrm{p}}^{(\kappa)}, D_{K_\mathrm{p}}^{(\kappa)}, \Pi_\mathrm{d}^{(\kappa)}\}$.

V. Four-Block IQC Controller Synthesis

For synthesis, the relation between Π and $\{N_{K_\mathrm{p}}, D_{K_\mathrm{p}}\}$ is nonlinear and (21) is non-convex. Hence, forming the main contribution of this letter, we propose an algorithm that iterates between finding a suitable IQC multiplier and a controller, similar to the DK-iterations in μ-synthesis.

A. IQC-Multiplier Iteration

Given $N_{K_\mathrm{p}}, D_{K_\mathrm{p}}$ and hence M, the multiplier iteration boils down to an IQC performance analysis problem and (21) can be rendered affine in Π, Π_d for a given performance multiplier family $\mathbf{\Pi}_\mathrm{d}$. See Section IV-C.

B. Controller Iteration

Given Π and let $\Pi_\mathrm{d} \in \mathbf{\Pi}_\mathrm{d}$. Rearrange (13) to obtain

$$\left(\frac{I}{M}\right)^* \left(\begin{array}{c|c} \tilde{\Pi}_{22} & \tilde{\Pi}_{12}^\top \\ \hline \tilde{\Pi}_{12} & \tilde{\Pi}_{11} \end{array}\right) \left(\frac{I}{M}\right) \prec 0 \quad \text{on } \mathbb{C}^0,$$
$$\forall \mathrm{p} \in \mathbb{P} \text{ and a } \Pi_\mathrm{d} \in \mathbf{\Pi}_\mathrm{d}, \tag{23}$$

where $\tilde{\Pi}_{22} = \mathrm{diag}(\Pi_{22}, \Pi_{\mathrm{d}22})$, $\tilde{\Pi}_{11} = \mathrm{diag}(\Pi_{11}, \Pi_{\mathrm{d}11})$ and $\tilde{\Pi}_{12} = \mathrm{diag}(\Pi_{12}^\top, \Pi_{\mathrm{d}12}^\top)$. Assuming $\tilde{\Pi}_{11} \succ 0$, (23) can be rendered affine in M, with M defined in (17), as follows

$$\begin{pmatrix} \tilde{\Pi}_{22} + \mathrm{He}\left(\tilde{\Pi}_{12} M\right) & M^* \\ M & -\tilde{\Pi}_{11}^{-1} \end{pmatrix} \prec 0 \quad \text{on } \mathbb{C}^0,$$
$$\forall \mathrm{p} \in \mathbb{P} \text{ and a } \Pi_\mathrm{d} \in \mathbf{\Pi}_\mathrm{d}. \tag{24}$$

Considering the data $\mathcal{D}_{N,\mathrm{p}_\ell}$, (24) is convex which, given a $\Pi \in \mathbf{\Pi}$, results in an optimal controller K_p.

C. IQC Synthesis Algorithm

To summarize the main contribution of the paper Algorithm 1 presents the controller synthesis procedure. Convergence of Π_d depends on the chosen family of performance multipliers $\mathbf{\Pi}_\mathrm{d}$. For example, if $\mathbf{\Pi}_\mathrm{d}$ defines the passivity multipliers (see [18]) then one iteration suffices.

The described algorithm constructs, at each iteration, pairs of multipliers and stabilizing controllers from fFRF data $\mathcal{D}_{N,\mathrm{p}_\ell}$. Although global convergence of Algorithm 1 is not guaranteed, separately, the multiplier and controller iterations are convex when considering the data $\mathcal{D}_{N,\mathrm{p}_\ell}$. Therefore, we can guarantee monotonic convergence because for $\{N_{K_\mathrm{p}}^{(\kappa)}, N_{K_\mathrm{p}}^{(\kappa)}\}$ given, there always exists a $\{\Pi^{(\kappa)}, \Pi_\mathrm{d}^{(\kappa)}\}$ with performance better than or equal to iteration $\kappa - 1$. Conversely, the same argument applies.

D. Controller Initialization

This section describes the initialization of the controller $\{N_{K_\mathrm{p}}, D_{K_\mathrm{p}}\}$ in Algorithm 1, forming Contribution I. The following theorem is based on our preliminary work [14, Theorem 1] for stability analysis of SISO systems.

Theorem 2: Let $\{N_{G_\mathrm{p}}, D_{G_\mathrm{p}}\}$ and $\{N_{K_\mathrm{p}}, D_{K_\mathrm{p}}\}$ denote an LCF and RCF of G_p and K_p, respectively, and D is as in (16). The following conditions are equivalent: For all $\mathrm{p} \in \mathbb{P}$,

4a) $D^{-1} \in \mathcal{RH}_\infty^{n_y \times n_y}$.

4b) There exists a multiplier $\Gamma_\mathrm{p} \in \mathcal{RH}_\infty^{n_y \times n_y}$ such that

$$\mathrm{He}\big(D(i\omega)\Gamma_\mathrm{p}(i\omega)\big) \succ 0, \text{ on } \mathbb{C}^0.$$

Proof ($\Rightarrow$): Assume 4a) and let $Q = D^{-1}$. This implies that the Bézout identity is satisfied for $X = N_{K_\mathrm{p}} Q$ and $Y = D_{K_\mathrm{p}} Q$. Hence, 4b) is satisfied by setting $\Gamma_\mathrm{p} = Q$ because $\mathrm{He}(\tilde{N}_{G_\mathrm{p}} X + \tilde{D}_{G_\mathrm{p}} Y) = I$ for all $\omega \in \mathbb{R} \cup \{\infty\}$.

($\Leftarrow$): Assume 4b) and let $U = D\Gamma_\mathrm{p}$. Note that $U, U^{-1} \in \mathcal{RH}_\infty^{n_y \times n_y}$, because 4b) implies that $D\Gamma_\mathrm{p}$ is bi-proper and has no right half-plane (RHP) zeros. Then $D = U\Gamma_\mathrm{p}^{-1}$ satisfies the Bézout identity, therefore $D^{-1} \in \mathcal{RH}_\infty^{n_y \times n_y}$. Thus, 4b) implies 4a). This completes the proof. ∎

Given the data $\mathcal{D}_{N,\mathrm{p}_\ell}$, Theorem 1 provides FDIs for the analysis of internal stability of (15). We can exploit this theorem to synthesize a stabilizing controller by absorbing Γ_p in the controller such that $\bar{N}_{K_\mathrm{p}} = N_{K_\mathrm{p}}\Gamma_\mathrm{p}$ and $\bar{D}_{K_\mathrm{p}} = D_{K_\mathrm{p}}\Gamma_\mathrm{p}$ such that $K_\mathrm{p} = \bar{N}_{K_\mathrm{p}}\Gamma_\mathrm{p}(\bar{D}_{K_\mathrm{p}}\Gamma_\mathrm{p})^{-1} = N_{K_\mathrm{p}} D_{K_\mathrm{p}}^{-1}$.

E. Controller Parameterization

Similar to our preliminary work [14], the controller is parameterized by orthonormal basis functions. Let

$$N_{K_\mathrm{p}}(s) = \sum_{i=0}^{n_N} W_i(\mathrm{p})\phi_i(s), \tag{25a}$$

$$D_{K_\mathrm{p}}(s) = \sum_{i=0}^{n_D} V_i(\mathrm{p})\varphi_i(s), \tag{25b}$$

where $\{\phi_i\}_{i=0}^{n_N}$ and $\{\varphi_i\}_{i=0}^{n_D}$ are sequences of basis functions with $\phi_0 = \varphi_0 = 1$, $n_D \geq n_N$, and coefficient functions

$$W_i(\mathrm{p}) = \sum_{\ell=1}^{m} \breve{W}_i^\ell \psi_\ell(\mathrm{p}), \quad V_i(\mathrm{p}) = \sum_{\ell=1}^{m} \breve{V}_i^\ell \psi_\ell(\mathrm{p}). \tag{26}$$

Here, the coefficient functions $W_i \in \mathbb{R}^{n_u \times n_y}$ and $V_i \in \mathbb{R}^{n_y \times n_y}$ are formed by a chosen functional dependence on the frozen scheduling variable p, e.g., affine, polynomial, or rational, characterized by the basis functions $\{\psi_\ell\}_{\ell=1}^m$.

The concept in this letter is that the global behavior of the controller $\mathcal{K}$ is tuned based on the local information $\mathcal{D}_{N,\mathrm{p}_\ell}$ and parameterization (25). For more information on the basis functions and the selection hereof, see [14].

VI. Results

Consider the two-mass-spring-damper system connected by a parameter-varying (e.g., position dependent) spring

$$\mathcal{G} : M\ddot{q}(t) + D\dot{q}(t) + K(p(t))q(t) = u(t), \tag{27}$$

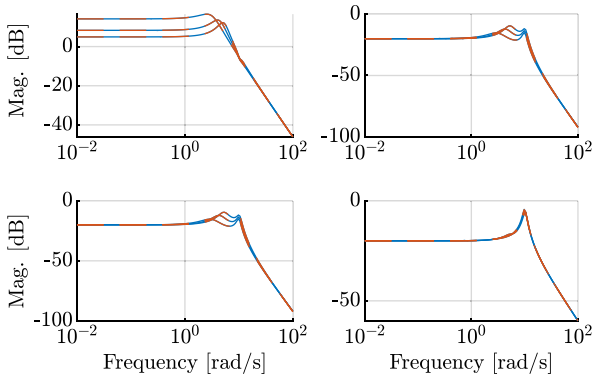

Fig. 3. Magnitude plots of the fFRFs of G_p for $\mathrm{p} \in \mathcal{P} = \{-1, 0, 1\}$ (blue) and the interpolated LPV model (dashed orange).

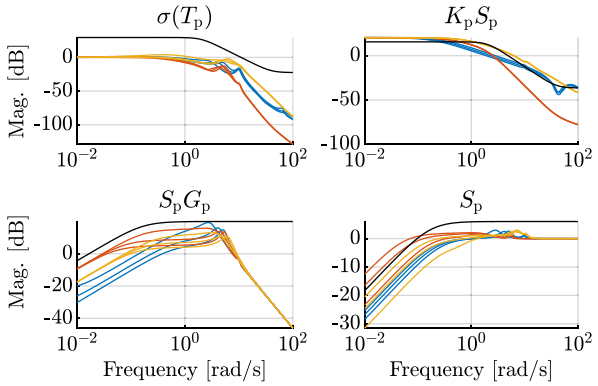

Fig. 4. Maximum singular values of the fFRFs of (4) with data-driven LPV (blue), LTI (orange) and model-based LPV (yellow) controllers, and weighting filters (black).

where $q \in \mathbb{R}^2$ denotes the position of the two masses, $u \in \mathbb{R}^2$ is the input signal, $y = q$ is the output signal and $p \in \mathbb{P}$ the scheduling variable, with $\mathbb{P} = [-1, 1]$. Here,

$$M = \begin{pmatrix} m_1 & 0 \\ 0 & m_2 \end{pmatrix}, \quad D = \begin{pmatrix} d+d_l & -d \\ -d & d+d_r \end{pmatrix},$$
$$K(p(t)) = \begin{pmatrix} k_0 & -k_0 \\ -k_0 & k_0+k_r \end{pmatrix} + \begin{pmatrix} k_1 & -k_1 \\ -k_1 & k_1 \end{pmatrix} p(t).$$

Fig. 3 shows the local behavior obtained at an equidistant grid $p(t) \equiv \mathrm{p} \in \mathcal{P} = \{-1, 0, 1\}$. We observe that the parameter-varying dynamics manifest itself in terms of a shift in the low-frequency gain and resonance frequencies.

The objective is to control the position of both masses simultaneously subject to variations in the spring stiffness. In terms of control design, the control objectives are specified in terms of weighting filters on the four-block map (4), shown in Fig. 4, where the goal is to minimize the $\mathcal{L}_2$-gain.

We synthesize (i) a data-driven LPV controller according to Algorithm 1, where N_{K_p} and D_{K_p} are parameterized by 4th order Laguerre basis functions with affine dependence on p. For comparison, we also design (ii) a data-driven LTI controller and (iii) a model-based LPV controller. The LTI controller is designed at the nominal operating point $\mathrm{p} = 0$, with N_{K_p} and D_{K_p} parameterized as in the data-driven LPV control design. To synthesize the model-based LPV controller, first local LTI models are estimated based on the fFRF data in Fig. 3 using frequency-domain subspace identification [19]. Next, an LPV model is interpolated through matching the input-output behavior of the local models and the considered

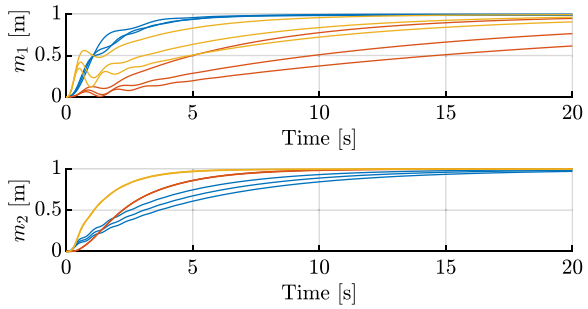

Fig. 5. Unit step responses of mass m_1 and m_2 for frozen $\mathrm{p} \in \mathcal{P}$, for the data-driven LPV (blue), LTI (orange) and model-based LPV (yellow) controllers, respectively.

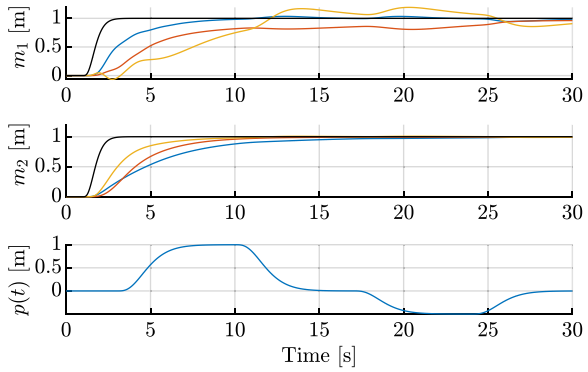

Fig. 6. Simulation results. The top and middle figures show the reference (black) and position of mass m_1 and m_2 for the LPV (blue), LTI (orange) and model-based LPV (yellow) controllers, respectively. The bottom plot shows the scheduling trajectory.

LPV model [20], see Fig. 3. Finally, a polytopic LPV controller is designed [9]. The controllers achieve $\mathcal{L}_2$-gains of 1.78, 2.41 and 1.78, respectively.

First, the tracking performance is evaluated locally for $\mathrm{p} \in \mathcal{P}$ in Fig. 5. The data-driven LPV controller has better performance for mass m_1, but has a slightly slower response for mass m_2 compared to the LTI and model-based designs. In Fig. 6, tracking results are shown for a time-varying scheduling trajectory. Similar conclusions can be drawn.

A possible explanation for the discrepancies is the available freedom in the controller parameterization that the data-driven LPV and LTI methods exploit to minimize the $\mathcal{L}_2$-gain. The performance of the model-based LPV controller depends on the quality of the LPV model. Hence accurate identification and interpolation is required to achieve good controllers. The results show the benefit of the data-driven LPV controller, which is able to increase the performance compared to the LTI controller, while avoiding a difficult LPV modeling and identification procedure. Note that we only guarantee stability and performance locally. Stability and performance of the nonlinear system are only guaranteed for sufficiently slow variations of the scheduling variable.

VII. Conclusion

This letter presents an approach to directly synthesize MIMO LPV controllers from frequency-domain data. The approach exploits a specific linear fractional representation of the four-block closed-loop interconnection such that it fits within the IQC framework. Coprime factorizations of the plant and controller are utilized to allow for a rational controller parameterization. The results are demonstrated by means of a simulation example.

References

[1] T. Oomen, "Advanced motion control for precision mechatronics: Control, identification, and learning of complex systems," *IEEJ J. Ind. Appl.*, vol. 7, no. 2, pp. 127–140, 2018.

[2] R. Pintelon and J. Schoukens, *System Identification: A Frequency Domain Approach*, 2nd ed. Hoboken, NJ, USA: Wiley, 2012.

[3] E. Grassi, K. S. Tsakalis, S. Dash, S. V. Gaikwad, W. MacArthur, and G. Stein, "Integrated system identification and PID controller tuning by frequency loop-shaping," *IEEE Trans. Control Syst. Technol.*, vol. 8, no. 5, pp. 842–847, Mar. 2001.

[4] S. Khadraoui, H. Nounou, M. Nounou, A. Datta, and S. P. Bhattacharyya, "A model-free design of reduced-order controllers and application to a DC servomotor," *Automatica*, vol. 50, no. 8, pp. 2142–2149, 2014.

[5] A. Karimi and C. Kammer, "A data-driven approach to robust control of multivariable systems by convex optimization," *Automatica*, vol. 85, pp. 227–233, Nov. 2017.

[6] A. Karimi, A. Nicoletti, and Y. Zhu, "Robust $\mathcal{H}_\infty$ controller design using frequency-domain data via convex optimization," *Int. J. Robust Nonlin Control*, vol. 28, no. 12, pp. 3766–3783, 2018.

[7] J. S. Shamma and M. Athans, "Gain scheduling: Potential hazards and possible remedies," *IEEE Trans. Control Syst. Mag.*, vol. 12, no. 3, pp. 101–107, Jun. 1992.

[8] R. Tóth, *Modeling and Identification of Linear Parameter-Varying Systems*. Berlin, Germany: Springer, 2010.

[9] C. Hoffmann and H. Werner, "A survey of linear parameter-varying control applications validated by experiments or high-fidelity simulations," *IEEE Trans. Control Syst. Technol.*, vol. 23, no. 2, pp. 416–433, Mar. 2015.

[10] S. Formentin, D. Piga, R. Tóth, and S. M. Savaresi, "Direct learning of LPV controllers from data," *Automatica*, vol. 65, pp. 98–110, Mar. 2016.

[11] A. Karimi and Z. Emedi, "$\mathcal{H}_\infty$ gain-scheduled controller design for rejection of time-varying narrow-band disturbances applied to a benchmark problem," *Eur. J. Control*, vol. 19, no. 4, pp. 279–288, 2013.

[12] T. Bloemers, R. Tóth, and T. Oomen, "Towards data-driven LPV controller synthesis based on frequency response functions," in *Proc. IEEE Conf. Decis. Control*, 2019, pp. 5680–5685.

[13] T. Bloemers, R. Tóth, and T. Oomen, "Frequency-domain data-driven controller synthesis for unstable LPV systems," in *Proc. 4th IFAC Workshop LPV Systems*, 2021, pp. 1–8.

[14] T. Bloemers, R. Tóth, and T. Oomen, "Frequency response data based LPV controller synthesis applied to a control moment gyroscope," 2021, *arXiv:2109.05774*.

[15] A. Rantzer and A. Megretski, "A convex parameterization of robustly stabilizing controllers," *IEEE Trans. Autom. Control*, vol. 39, no. 9, pp. 1802–1808, Sep. 1994.

[16] A. Megretski and A. Rantzer, "System analysis via integral quadratic constraints," *IEEE Trans. Autom. Control*, vol. 42, no. 6, pp. 819–830, Jun. 1997.

[17] J. Veenman, *A General Framework for Robust Analysis and Control: An IQC Based Approach*. Berlin, Germany: Logos Verlag, 2015.

[18] J. Veenman, C. W. Scherer, and H. Köroğlu, "Robust stability and performance analysis based on IQC," *Eur. J. Control*, vol. 31, pp. 1–32, Sep. 2016.

[19] T. McKelvey and M. Gibanica, "FSID-A frequency weighted MIMO frequency domain identification and rational matrix approximation method for Python, Julia and Matlab," in *Proc. 19th IFAC Symp. Syst. Identif.*, 2021, pp. 403–408.

[20] D. Vizer, G. Mercere, O. Prot, E. Laroche, and M. Lovera, "Linear fractional LPV model identification from local experiments: An $\mathcal{H}_\infty$-based optimization technique," in *Proc. 52nd IEEE Conf. Decis. Control*, 2013, pp. 4559–4564.